Atlas-Based Segmentation of Brain Structures in Temporal Lobe Epilepsy Using Optimized Voxel-Based Morphometry

Matineh Shaker[1], Hamid Soltanian-Zadeh[1-3]

[1] Control and Intelligent Processing Center of Excellence, Department of Electrical and Computer Engineering, University of Tehran, Tehran, Iran
m.shaker@ece.ut.ac.ir, hszadeh@ut.ac.ir

[2] School of Cognitive Sciences, Institute for Studies in Theoretical Physics and Mathematics (IPM), Tehran, Iran

[3] Image Analysis Lab., Department of Radiology, Henry Ford Hospital, Detroit, Michigan, USA
hamids@rad.hfh.edu

Abstract

The purpose of this study was to segment the brain structures in temporal lobe epilepsy (TLE) using 3D T1-weighed magnetic resonance images (MRI). Twelve patients with average age of 43 and standard deviation of 12 years were studied. We used specific preprocessing stages through optimized voxel-based morphometry (VBM) with additional spatial normalization steps to obtain more accurate results. Specific template creation, excluding nonbrain voxels by morphological operations, image registration, gray matter (GM) segmentation, and correction for volume changes are different stages of spatial normalization in optimized VBM. All of the gray matter voxels were labeled using an anatomical atlas to create individual regions for each of the brain structures. In our study, we examined hippocampus, amygdala, and entorhinal cortex which are most affected by TLE. The proposed approaches are evaluated by comparing automatic and expert's segmentation results and confirming their similarity.

Keywords

Voxel-based morphometry, Temporal lobe epilepsy, Image segmentation, Atlas-Based Labeling

1. Introduction

Many neurodegenerative diseases exhibit volume and shape changes in specific brain regions. Quantitative volume measurements of the brain structures are useful for the diagnosis and prognosis of neurological disorders [1,2]. These studies have clinical values in diagnosis stage, decision about surgeries and treatment evaluations. Manual delineation of brain structures suffer from difficulties of defining anatomical landmarks and boundaries, as well as obtaining results with low reproducibility and objectivity.

For evaluating the volume changes of these structures, first we should segment them from 3D MR images. The accuracy of segmentation procedure has a great impact on the final results for volumes of the structures. The volumes of structures will help us to find abnormal side of the brain by comparing the structures' volumes in the two sides of the brain.

In this study, we focus on automatic segmentation of brain structures from MR images of temporal lobe epilepsy (TLE) patients. Volumetric MRI studies of brain structures in TLE have showed brain abnormalities associated with this disease [3]. Among all of the brain structures, those in the temporal lobe of the brain are most affected by TLE. We develop automatic methods for the segmentation of the hippocampus, amygdala, and entorhinal cortex which are among the most challenging structures in the brain to segment.

First, preprocessing stages are applied to the image data. These steps are the ones used for optimized voxel-based morphometry (VBM), which is an automated technique that performs voxel-wise statistical analysis of MR images [4]. Our method includes spatial normalization, gray matter (GM) segmentation, exclusion of non-brain voxels, and compensation of spatial normalization effects. Then, all of the gray matter voxels are labeled using an anatomical atlas to create individual regions for each of the brain structures. By making the maximum probability atlas, corresponding voxels of hippocampus, amygdala, and entorhinal cortex are obtained.

The scheme is evaluated through two experiments. First of all, we measure the similarity between automatic and expert's segmentation results through Dice's coefficient and gain satisfactory results. Second, we compared similarity coefficients of our proposed method with those obtained by standard methods of preprocessing of data.

Novel contributions of this work are two-fold. First, we use a specific atlas-based procedure for segmentation of brain structures. Secondly, we segment the entorhinal cortex automatically. This structure is an important memory center in the brain and is one of the first areas to be affected in neurodegenerative diseases like Alzheimer's and TLE. Thus, developing automatic methods for segmentation of this structure is a valuable work. To our knowledge, none of the previous studies segmented this structure automatically.

The present paper is organized as follows. In Section 2, the specifications of data and image acquisition protocol are described. Also, we discuss about the preprocessing stages and our atlas-based labeling method. Section 3 presents the segmentation results and evidences for their accuracy. Finally, section 4 concludes the paper.

2. Materials and Methods

2.1. Image Acquisition and Subjects

Magnetic resonance images were acquired using a General Electric 3 Tesla Signa system (GE Medical System, Milwaukee, WI). All patients underwent coronal T1-weighted MRI study using a spoiled gradient-echo (SPGR) sequence with $TR/TI/TE = 7.6/1.7/500ms$, flip angle = $20^{\mathbf{0}}$, field of view (FOV) = $200\times200mm^2$, matrix size = 256×256, pixel size = $0.781\times0.781mm^2$, and slice thickness = $2.0mm$.

Twelve patients were included in this study (6 female, 6 male). They are adults with an age average and standard deviation of 43 and 12 years, respectively.

2.2. Spatial Processing

In this section, we first describe the stages of standard method for preprocessing of the structural data, which are also used for standard VBM. Then, we mention the need for using modified techniques and describe the steps of optimized VBM.

2.2.1. Standard VBM

The standard VBM method consists of multiple stages. At its simplest case, preprocessing of data in VBM involves spatially normalizing images into a common stereotactic space. This is obtained by registering each of the images to the same template image by estimating the 12-parameter affine transformation. This is followed by segmentation of GM from MR images based on voxel intensities. The next step is smoothing the GM segments with Gaussian kernels. By the central limit theorem, smoothing the data will render the errors more normal in their distribution and ensure the validity of inferences based on parametric tests [5].

However, there were some problems with the standard VBM that led to establishing modified procedures [6],[7]. Evaluation of segmented images from standard VBM protocol shows that some small areas in GM segmented images like scalp fat are often misclassified as gray matter. Besides, if one subjects' structures has a very different volume compared to the template, then its volume changes dramatically during the warping step. So, the obtained volume is not correct. The method addressed in the next section will reduce these undesirable effects.

2.2.2. Optimized VBM

For reducing the effect of nonbrain regions on GM segmented images, some additional preprocessing steps can be applied to exclude nonbrain voxels prior to normalization and subsequent segmentation.

A so-called optimized VBM was introduced in [8], which includes automated brain extraction steps as well as correction for volume changes. The steps of this method are as follows.

Template Creation. All of the structural images are normalized to a stereotactic space. Then they are segmented to GM/WM partitions. This, segmentation is performed by the probability maps, used as Bayesian priors. After smoothing the segmented images, the final GM/WM templates are created by averaging all the smoothed segmented normalized images. This stage is the same as that of standard VBM protocol.

Exclude nonbrain voxels. All of the segmented gray matter images are eroded to remove nonbrain voxels from skull, scalp, and venous sinuses. This erosion is followed by conditional dilation. The obtained images are extracted gray matter and white matter partitions in the stereotactic space.

Normalization. The extracted GM/WM partitions are normalized to gray matter and white matter templates obtained by standard VBM.

Modulation. Spatial normalization may cause some specific regions of the brain to grow and other regions to shrink. This effect can be compensated by multiplying voxel values of spatially normalized GM images by relative volume of GM before and after normalization. Indeed, this work is a modulation procedure. The changes of regions in the normalized image in relation to the original image make a deformation field. The gradient of this deformation field is its Jaccobian matrix and consists of the following matrix in the 3D space.

$$\begin{bmatrix} \frac{dx}{dx'} & \frac{dx}{dy'} & \frac{dx}{dz'} \\ \frac{dy}{dx'} & \frac{dy}{dy'} & \frac{dy}{dz'} \\ \frac{dz}{dx'} & \frac{dz}{dy'} & \frac{dz}{dz'} \end{bmatrix} \quad (1)$$

where $[x\ y\ z]$ and $[x'\ y'\ z']$ are the vectors of coordinate in the original and normalized images, respectively.

Thus, we can use the determinant of Jaccobian matrix as a measure of relative volumes of the GM before and after normalization.

2.3. Atlas-Based Segmentation

To obtain a rough segmentation of brain structures, each individual gray mater voxel is labeled based on the MNI atlas and the transformation matrix gained in preprocessing step. Then, by computing the voxel by voxel average of the same structure label from a group of subjects, statistical probability anatomy maps are created. Finally, the label of the most probable structure is stored at each voxel of the maximum probability atlas. We extract the corresponding voxels of the hippocampus, amygdala, and entorhinal cortex and obtain three-dimensional segmentation of these structures.

3. Data Analysis and Results

Preprocessing of structural MRI data was performed using SPM5 (Wellcome Department of Imaging Neuroscience, London, UK; www.fil.ion.ucl.ac.uk). We accomplished both standard and optimized VBM methods for investigation of data using the steps described in the previous section. The images were normalized to the Montreal Neurological Institute (MNI) T1-weighted template using 12 parameter affine transformation. The algorithm works by minimizing the sum of the squared errors between each image and template. Also, the images were corrected for the bias effects. The MR images are usually affected by smooth artifacts that are not problems for visual inspection, but can make problems for automated procedures. Fig. 1 shows the MR images after and before Intensity non-uniformity correction.

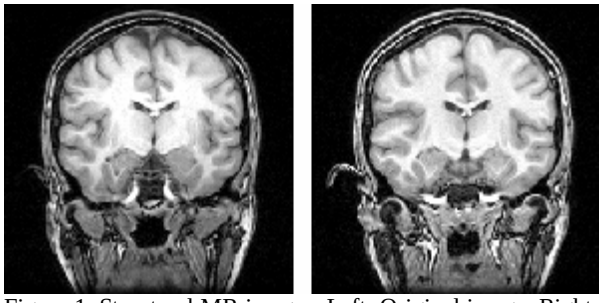

Figure 1. Structural MR images. Left: Original image, Right: Image after intensity non-uniformity correction.

After segmentation of GM and extracting brain by morphological operations, a $3\text{mm} \times 3\text{mm} \times 3\text{mm}$ full-width half-maximum (FWHM) isotropic Gaussian kernel is used to smooth the GM partitions for subsequent statistical analysis. The GM images obtained by standard and optimized VBM are shown in Fig. 2. It is clear that some nonbrain regions are removed using the optimized method. Also, some WM regions that are misclassified as GM, are removed in optimized method (see arrows).

Then, all of the gray matter voxels are labeled using an anatomical atlas and the transformation matrix obtained in the normalization process. This creates individual anatomical atlases for each of the structural images. After transforming the individual atlases into stereotaxic space, average of same structure label derived from individual atlases are computed. Finally, the corresponding voxels of the desires structures are extracted by assigning the label of most probable structure at each voxel of the maximum probability atlas.

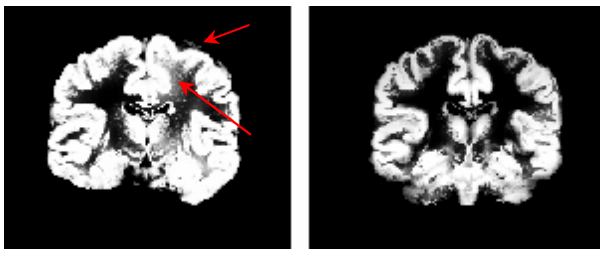

Figure 2. GM partitions. Left: Standard VBM, Right: Optimized VBM.

We have applied the proposed method to the coronal MR images to segment the hippocampus, amygdala, and entorhinal cortex. Figures 3-5 show the segmentation results. We use manually segmented images by an expert to evaluate the automatic segmentation results.

To obtain a quantitative measure, we have calculated the Dice's coefficient as a similarity measure:

$$s = \frac{2|X \cap Y|}{|X| + |Y|} \quad (2)$$

where X and Y are the sets that we want to measure their similarity. For measuring the similarity between automatic segmentation and expert's segmentation, we used the following measure:

$$s = \frac{2n_{overlap}}{n_{automatic} + n_{manual}} \quad (3)$$

where $n_{automatic}$ is the number of pixels in the structure segmented automatically, n_{manual} is the number of pixels in the structure segmented manually, and $n_{overlap}$ is the number of pixels that belong to both of them. We have measured this coefficient for each of the three structures. For evaluation of the results, the brain slices that include these structures have been selected from MRI studies of each of the twelve

subjects. Table 1 presents the mean and standard deviation of the similarity measures between our automatic segmentation method and expert's segmentations for the twelve subjects. Also, we have calculated the similarity measures between the manual segmentation and the atlas based segmentation proceed by standard VBM method. These results are also shown in Table 1 and reflect the superiority of our proposed method. Also, we computed the volumes of hippocampus, amygdala, and entorhinal cortex in the two sides of the brain, for all of the patients. The results are presented in Table 2.

Table 1. Mean and standard deviation of similarity measures for the left and right hippocampus, amygdala, and entorhinal cortex, as segmented by the automatic method and the expert for brain slices that include these structures, acquired from 12 subjects. The optimized method is our proposed atlas-based segmentation with additional preprocessing stages.

	Aveage ± *std* **Optimized Method**	*Aveage* ± *std* **Standard Method**
Right Hippocampus	0.89 ± 0.04	0.86 ± 0.05
Left Hippocampus	0.90 ± 0.03	0.86 ± 0.04
Right Amygdala	0.84 ± 0.04	0.81 ± 0.05
Left Amygdala	0.87 ± 0.06	0.85 ± 0.06
Right entorhinal cortex	0.80 ± 0.05	0.78 ± 0.04
Left entorhinal cortex	0.79 ± 0.05	0.75 ± 0.06
Overall	**0.85 ± 0.04**	**0.82 ± 0.05**

4. Conclusion

In the present work, we used the integration of a specific atlas-based labeling method and optimized VBM to segment hippocampus, amygdala, and entorhinal cortex in 3D MR images of patients with TLE.

Obtaining a precise segmentation of these structures, is the first and most important step in quantitative evaluation of the brain structures in TLE. Volumetric MRI studies of the brain structures have clinical values in diagnosis stage, decision about surgeries, and treatment evaluations.

The accuracy of segmentation procedure will lead to precise results for volumes of structures. Having the volumes of structures will help us to discover the side of seizure by comparing the structures' volumes in the two sides of the brain.

When segmenting an anatomical structure, having priori information about the shape of the structure and its boundaries can significantly improve the final segmentation results. Priori information about the structures was obtained by registering the images to an atlas and labeling the voxels accordingly. The proposed method has successfully segmented the entorhinal cortex which is a very small and difficult-to-segment structure in the coronal view of the brain.

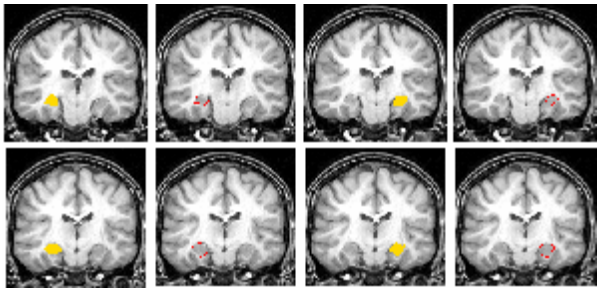

Figure 3. Automatic and expert's hippocampus segmentation results for two different slices on the coronal view. First and third columns show automatic segmentation, while second and fourth columns show manual (expert's) segmentation results.

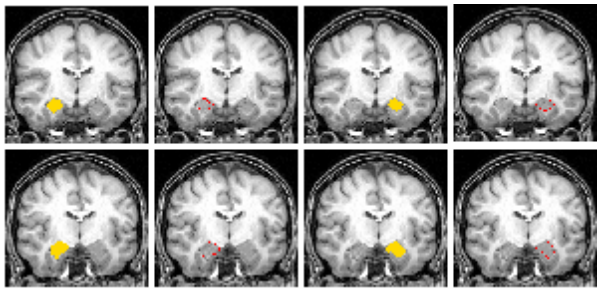

Figure 4. Automatic and expert's amygdala segmentation results for two different slices on the coronal view. First and third columns show automatic segmentation, while second and fourth columns show manual (expert's) segmentation results.

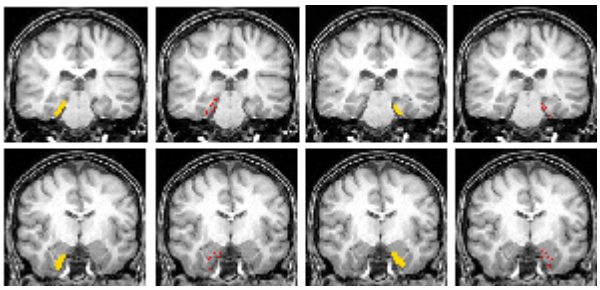

Figure 5. Automatic and expert's Entorhinal Cortex segmentation results for two different slices on the coronal view. First and third columns show automatic segmentation, while second and fourth columns show manual (expert's) segmentation results.

Acknowledgment

The authors would like to thank Dr. Kourosh Jafari-Khouzani for his invaluable help with data organization and helpful discussion of the results.

Table 2. Volumes of hippocampus, amygdala, and entorhinal cortex for all of the patients in the two sides of the brain.

Structure / Subject	Left Hippocampus	Right Hippocampus	Left Amygdala	Right Amygdala	Left Entorhinal	Right Entorhinal
Patient #1	3.02	3.43	1.68	2.12	2.32	2.51
Patient #2	3.44	3.25	2.23	2.57	2.48	2.68
Patient #3	3.28	2.84	2.25	2.34	2.12	1.87
Patient #4	2.93	3.37	1.55	1.37	1.96	1.62
Patient #5	3.54	3.72	2.32	2.65	2.56	2.71
Patient #6	3.21	2.79	1.97	1.63	1.87	1.43
Patient #7	2.92	2.58	1.53	1.83	2.23	2.45
Patient #8	3.79	3.38	2.28	2.42	1.81	1.56
Patient #9	3.24	2.71	2.33	1.89	1.78	1.9
Patient #10	3.03	2.66	1.84	1.58	2.38	2.04
Patient #11	2.69	2.50	1.71	1.83	2.54	2.39
Patient #12	3.22	3.53	2.21	2.64	2.31	2.55

References

[1] S. Duchesne, N. Bernasconi, A. Bernasconi and D.L. Collins, "MR-based neurological disease classification methodology: Application to lateralization of seizure focus in temporal lobe epilepsy," *NeuroImage*, vol. 29, pp. 557-566, 2006.

[2] N. Bernasconi, S. Duchesne, A. Janke, "Whole-brain voxel-based statistical analysis of gray matter and white matter in temporal lobe epilepsy," *Neuroimage*, vol. 23, pp. 717–723, 2004.

[3] L. Bonilha, C. Rorden, G. Castellano, F. Cendes, and L. M. Li, "Voxel-based Morphometry of the thalamus in patients with refractory medial temporal lobe epilepsy," *Neuroimage*, vol. 25, pp.1016–1021, 2005.

[4] J. Ashburner, K. J. Friston, "Voxel-based morphometry-The methods," *NeuroImage*, vol. 11, pp. 805– 821, 2000.

[5] J. Ashburner, K. Friston, "Comments and Controversies: why voxel-based morphometry should be used," *NeuroImage*, vol. 14, pp. 1238-1243, 2001.

[6] keller, S., Wilke, M., Wieshmann, U., Sluming, V., and Roberts, N., " Comparison of standard and optimized voxel-based morphometry for analysis of brain changes associated with temporal lobe epilepsy" *NeuroImage* vol. 23, pp. 860-868, 2005.

[7] keller, S., Wilke, M., Wieshmann, U., Sluming, V., and Roberts, N., " Comparison of standard and optimized voxel-based morphometry for analysis of brain changes associated with temporal lobe epilepsy" *NeuroImage* vol. 23, pp. 860-868, 2005.

[8] C. D. Good, I. S. Johnsrude, J. Ashburner, N. A. R. Henson, K. J. Friston, R. Frackowiak, "A voxel-based morphometric study of aging in 465 normal adult human brains," *NeuroImage*, vol. 14, pp. 21-36, 2001.